



Research



Cite this article: Fernandes AE, Pol D, Rauhut OWM. 2024 The oldest monofenestratan pterosaur from the Queso Rallado locality (Cañadón Asfalto Formation, Toarcian) of Chubut Province, Patagonia, Argentina. *R. Soc. Open Sci.* **11**: 241238.

<https://doi.org/10.1098/rsos.241238>

Received: 25 July 2024

Accepted: 23 September 2024

Subject Category:

Earth and environmental science

Subject Areas:

palaeontology, palaeontology, geology

Keywords:

Pterosauria, Monofenestrata, Jurassic, Toarcian, Patagonia, Argentina

Author for correspondence:

Alexandra E. Fernandes

e-mail: fernandes@snsb.de

Electronic supplementary material is available online at <https://doi.org/10.6084/m9.figshare.c.7550725>.

The oldest monofenestratan pterosaur from the Queso Rallado locality (Cañadón Asfalto Formation, Toarcian) of Chubut Province, Patagonia, Argentina

Alexandra E. Fernandes^{1,2}, Diego Pol³ and Oliver W. M. Rauhut^{1,2,4}

¹SNSB, Bayerische Staatssammlung für Paläontologie und Geologie, Richard-Wagner-Straße 10, 80333 Munich, Germany

²Department of Earth and Environmental Sciences, Ludwig-Maximilians-University, Theresienstraße 41, 80333 Munich, Germany

³CONICET, Museo Argentino de Ciencias Naturales 'Bernardino Rivadavia', Avenida Patricias Argentinas 480, C1405 Ciudad Autónoma de Buenos Aires, Argentina

⁴GeoBioCenter, Ludwig-Maximilians Universität, Richard-Wagner-Straße 10, 80333 Munich, Germany

AEF, 0000-0003-4336-8318

As the first group of tetrapods to achieve powered flight, pterosaurs first appeared in the Late Triassic. They proliferated globally, and by the Late Jurassic through the Cretaceous, the majority of these taxa belonged to the clade Monofenestrata (which includes the well-known Pterodactyloidea as its major subclade), typified by their single undivided fenestra anterior to the orbit. Here, a new taxon *Melkamter pateko* gen. et sp. nov., represented by the specimen MPEF-PV 11530 (comprising a partial cranium and associated postcranial elements), is reported from the latest Early Jurassic (Toarcian) locality of Queso Rallado (Cañadón Asfalto Formation) and referred to the clade Monofenestrata, increasing our previously known taxonomic and geographic representations, and temporal range for this clade. This occurrence marks the oldest record of Monofenestrata globally and helps to shed critical light on the evolutionary processes undergone during the 'non-pterodactyloid'-to-pterodactyloid transition within the Pterosauria. In addition, another single isolated tooth from the same locality shows ctenochasmatid affinities. These finds

further elucidate the still-poor Gondwanan Jurassic pterosaur fossil record, underscoring that most of our current ideas about the timing and modes of pterosaur evolution during that period are largely based on (and biased by) the pterosaur fossil record of the Northern Hemisphere.

1. Introduction

Pterosaurs were the first clade of actively flying tetrapods and were highly successful during the Mesozoic, achieving a global distribution from the Triassic to the Cretaceous. Over that time, the pterosaur bauplan transitioned from the basal nonmonofenestratan ‘non-pterodactyloid’ body style to that of the more derived pterodactyloids [1–4]. This evolutionary event has become better understood in recent years, with the recognition of the clade Darwinoptera, which have been largely considered as ‘intermediate’ monofenestratans that show a morphological array of attributes during this transition, combining plesiomorphic characters of ‘non-pterodactyloids’ with pterodactyloid features [5,6]. Rather than exhibit intermediate character states, the evolutionary pathway of transitional pterosaurs often exhibited seemingly cherry-picked traits, adopting both ancestral and derived states simultaneously, which typifies mosaic evolution [6]. Within Monofenestrata (the clade comprised of Darwinoptera and Pterodactyloidea), members of Wukongopteridae (Darwinoptera to the exclusion of *Pterorhynchus*) exhibit characters from both basal non-pterodactyloids and derived pterodactyloids: a confluence of the nares and antorbital fenestra; a posteriorly inclined quadrate; a glenoid located on the scapula; reduced cervical ribs and a wing metacarpal about half the length of the first wing phalanx; still retaining an elongated tail enclosed by rod-like bony extensions made by the zygapophyses. Pterodactyloids then went on to adapt even more dramatically elongated crania and cervical vertebrae, a further reduction or loss of cervical ribs, elongation of the metacarpus, reduced tails, and a highly reduced or absent fifth toe. However, sound examples of these intermediate fossil forms are rare, particularly on the global scale, and therefore it has made challenging the process of identifying the mechanisms that underpin these transitions [6]. Although these changes are presumed to have had their evolutionary origins during the early–middle Jurassic time period, the evolutionary pathway towards pterodactyloids is still largely unknown [2]. Poor availability of geochronologic exposures from this time period, inadequate field sampling, and low bone preservation rates all hinder the understanding of this critical phase in which body plans changed so drastically [7,8].

The Mesozoic pterosaur record is abundant in the Northern Hemisphere, whereas the record in the Southern Hemisphere is comparatively more scarce [9–12]. With the possible exclusion of the Argentinian *Allkaruen koi* Codorníu *et al.* (2016) [13], non-pterodactyloid monofenestratan pterosaurs have thus far only been recovered from the Northern Hemisphere, namely the UK [5,14], Germany [15–17] and China (e.g. [6,18,19]), where they first appeared during the Bathonian [5,14]. The apparent success of these monofenestratan forms and their pterodactyloid descendants went on to supplant the rhamphorhynchid body style (which disappeared in the Early Cretaceous [4,20]), surviving through to the end-Cretaceous extinction. However, there is still a dearth of knowledge about non-pterodactyloid monofenestratans, specifically in terrestrial sedimentary settings [1,5,7,21,22].

Pterosaur records from Gondwana are especially meagre for the Jurassic [9,23], although Argentina itself contains fossil-yielding exposures from the Late Triassic to the Late Cretaceous (Toarcian–Coniacian), a span of over approx. 85 Ma [10,24]. Specimens have been recovered from at least 13 different fossil localities overall [25,13,23,26,27], but mainly come from two geographical regions: central–western Argentina (San Juan and San Luis Provinces) and Patagonia [13]. Most of the Jurassic records come from the highest parts of the Jurassic, with the exception of the latest Early Jurassic Cañadón Asfalto Formation [28]. This unit, which is exposed in the province of Chubut, comprises the bone-bed containing *Alkaruen koi*, a Breviquartossan (the least inclusive clade containing *Rhamphorhynchus muensteri* Goldfuß [29] and *Quetzalcoatlus northropi* Lawson (1975) [30,31]), which is based on exceptional three-dimensionally preserved cranial and postcranial material [13,32]. Otherwise, only three other pterosaur taxa have been described from the Jurassic of South America thus far: *Herbstosaurus pigmaeus* Casamiquela (1975) [33], and *Wenupteryx uzi* Codorníu and Gasparini (2013) [34], from the Tithonian Vaca Muerta Formation of Neuquén, Argentina, and *Tucuaedactylus luciae* Soto *et al.* (2021), from the latest Jurassic Tacuarembó Formation of Uruguay.

Here, new pterosaur fossils are presented from the locality of Queso Rallado of the Cañadón Asfalto Formation of Chubut Province, one of them representing a diagnosable new taxon, based on

associated remains of preserved cranial and postcranial material. This specimen includes a partial cranium (including part of the premaxilla–maxilla–jugal–lacrima–postorbital–squamosal–quadratojugal–quadrate complex) and a few postcranial remains (four vertebrae and a manual metacarpal), and its anatomy shows clear monofenestratan affinities. The second specimen is limited to an isolated tooth that presents derived similarities with ctenochasmatid pterodactyls.

2. Geological and palaeontological setting

The Cañadón Asfalto Formation crops out in the northern central part of Chubut Province, Argentina. It is part of the sedimentary infill of the Cañadón Asfalto Basin, a large semigraben structure on central Patagonia that opened with the beginning of the South Atlantic in the Early Jurassic [35]. It belongs to the megasequence 1 of this infill, which represents the synrift phase of the basin, and conformably overlies the mainly volcanic Lonco Trapial Formation. The Cañadón Asfalto Formation is mainly composed of lacustrine shales, biogenic limestones and mudstones, with intercalated basaltic flows and pyroclastic deposits in the base, and fanglomerates and conglomerates in some sections [35–37]. The age of the formation has long been debated. Originally considered to be of Callovian–Oxfordian age (e.g. [38]), new biostratigraphic and radiometric dates have recently indicated an uppermost Early (Toarcian) to early–Middle Jurassic (Aalenian–Bajocian) age for this unit [39,40]. Even more recent radiometric dates, however, indicate that most (if not all) of the formation may be Toarcian in age [28,41,42].

The Queso Rallado locality is located approx. 5.5 km northwest of the village of Cerro Córdo (figure 1) in the area of the mid-course of the Río Chubut. The fossiliferous level is a 0.8 m thick carbonatic and partially silicified mudstone within the lower part of the section of the Cañadón Asfalto Formation. The exact stratigraphic correlation of the outcrops at Queso Rallado awaits publication, but a Toarcian age is considered the age of the fossiliferous level [40]. The fossiliferous strata at Queso Rallado have yielded a rich microvertebrate fauna of both aquatic and terrestrial animals. The fauna includes so far undescribed fishes, amphibians, crocodiles, pterosaurs and theropod teeth, as well as the turtle *Condorchelys antiqua* Sterli (2008) [44], the rhynchocephalian *Sphenocondor gracilis* Apesteguía, Gómez & Rougier (2012) [45], the heterodontosaurid ornithischian *Manidens condorensis* Pol, Rauhut & Becerra (2011), teeth of sauropod dinosaurs [46,47] and the mammaliaforms *Asfaltomylos patagonicus* Rauhut *et al.* (2003), *Condorodon spanios* Gaetano & Rougier (2012) [48], *Henosferus molus* Rougier *et al.* (2007) [49] and *Argentoconodon fariasi* Gaetano & Rougier (2011) [50]. Other outcrops of the Cañadón Asfalto Formation have yielded the anuran *Nothobatrachus reigi* Báez & Nicoli (2008), the sauropod dinosaurs *Volkheimeria chubutensis* Bonaparte (1978) [38], *Patagosaurus fariasi* Bonaparte (1978) [38] and *Bagualia alba* Pol *et al.* (2020), the theropod dinosaurs *Piatnitzkysaurus floresii* Bonaparte (1978) [38], *Condorraptor currumili* Rauhut (2005) [51], *Eoabelisaurus mefi* Pol & Rauhut (2012) and *Asfaltovenator vialidadii* Rauhut & Pol (2019) [52], as well as the pterosaur *Allkaruen koi* Codorniu *et al.* (2016) [13].

3. Material and methods

The main specimen described herein comes from the microvertebrate locality of Queso Rallado [25]. It was found by mechanically breaking blocks that were recovered from the fossiliferous layer, during which the partial skull was split. Subsequently, the specimen was mechanically prepared, revealing additional bones originally still covered in matrix. Although the bones were not found in articulation, they were found in close association, and consist of a partial skull, four dorsal vertebrae, one long bone and two associated teeth. All measurements were taken with digital callipers. In addition, an isolated ctenochasmatid (?) tooth was recovered in the same locality (but from an unknown horizon), which is also reported upon. The specimens are housed at the Museo Paleontológico ‘Egidio Feruglio’ (MPEF) in Trelew (Province of Chubut Province), Argentina under the collection numbers MPEF-PV 11530 a–c and MPEF-PV 2549[2012].

CT scans were performed at the three-dimensional Imaging Lab of the University of Tübingen, using a Nikon XT H 320 with a tungsten reflection target with a maximum voltage of 225 kV. This resulted in a stack of 2714 projections (voxel size = 0.113606). The data derived from the CT scan were segmented manually (Image Segmentation) with the software Avizo v9.2 (Thermo Fisher Scientific, MA, USA), using the brush function and interpolation, and rendered using the open-source software Blender. All CT files are available at <https://www.morphosource.org/projects/000495959>.

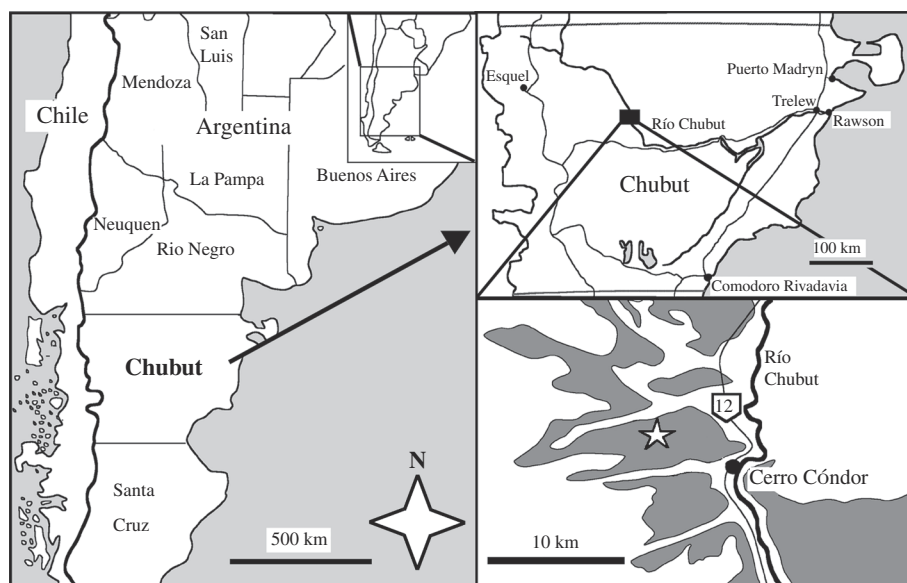


Figure 1. Map of the Queso Rallado locality (marked with a star) within the Chubut Province of Argentina, with the Cañadón Asfalto Formation shaded in dark grey (modified from [43]).

Phylogenetic analysis was conducted in TNT version 1.6 [53,54] using two matrices: the matrix of Fernandes *et al.* [55], which is in turn based on the matrix of Andres [56], and the matrix of Martin-Silverstone *et al.* [5]. In both matrices, we added the new taxon, checked the codings for *Allkaruen koi* (*Dimorphodon koi* in the matrix of Andres (2021) [56]; we changed the name back to *Allkaruen* in our matrix), based on our own observations, and added an additional character, the presence or absence of an ascending process of the maxilla. Thus, the final matrix based on Fernandes *et al.* [55] had 181 terminal taxa scored for 276 characters (51 continuous and 225 discrete; ordered and unordered), and the one modified from Martin-Silverstone *et al.* [5] had 70 terminal taxa scored for 136 characters (ordered and unordered). The data matrices are available in the electronic supplementary material, and also at <http://morphobank.org/permalink/?P4589>. Both matrices were analysed under equal and implied weights (with $k = 12$ [57]) using a traditional search with 2000 replicates, followed by TBR branch swapping on trees in memory. Reduced consensus methods were used to improve the resolution of the final results, using the pcrprune command [57,58].

4. Nomenclatural acts

The electronic edition of this article conforms to the requirements of the amended International Code of Zoological Nomenclature, and hence the new names contained herein are available under that Code from the electronic edition of this article. This published work and the nomenclatural acts it contains have been registered in ZooBank, the online registration system for the ICZN. The electronic edition of this work was published in a journal with an ISSN and has been archived and is available from the following digital repositories: PubMed Central and LOCKSS. LSID:

5. Results

5.1. Systematic palaeontology

PTEROSAURIA Owen, (1842) [59]

MONOFENESTRATA Lü *et al.* (2010) [6] *sensu* Andres *et al.* (2014) [1]

Genus *Melkamter*, **gen. nov.**

5.1.1. Etymology

Genus name '*Melkamter*' from the native Tehuelche word 'mel' meaning (in Spanish/English) 'ala/wing' and 'kamter' meaning 'lagarto grande/big lizard' (after the original translation of 'pterosaur' as 'winged lizard'); the species epithet '*pateko*' is derived from 'pate' meaning 'rallado/rasped' and 'ko' meaning 'conjunto de huesos/set of bones', an ode to both to the site of Queso Rallado, and the fractured preservational state of the fossil (translations from [60]).

5.1.2. Holotype

MPEF-PV 11530 (Museo Paleontológico Egidio Feruglio, Trelew, Argentina), consisting of at least a partial cranium (with counterslab) and two associated teeth, four dorsal vertebrae, one metacarpal (either I, II or III) and other bone fragments⁵.

5.1.3. Type locality and hHorizon

Locality Queso Rallado, close to Cerro Cóndor, northern central Chubut Province, Argentina. Lower section of the Cañadón Asfalto Formation, latest Early Jurassic, Toarcian [28,40].

5.1.4. Diagnosis

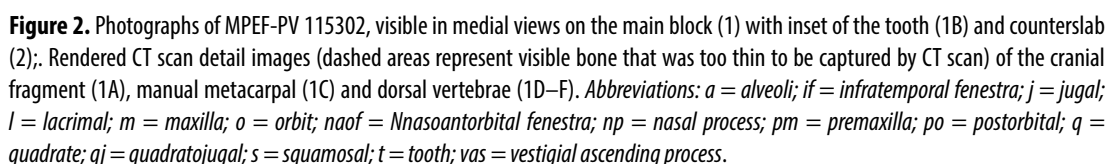
Non-pterdactyloid monofenestratan with a confluent naris and anteorbital fenestra and quadrate inclined at about 120°. Autapomorphies include: the presence of a small vestigial ascending process in the maxilla that does not reach the nasal or lacrimal dorsally; a maxillary body anterior to the vestigial ascending process that is higher than a posterior portion, with both portions divided by the vestigial ascending process delimited by a marked step; lacrimal and posterior processes of the jugal offset at about 55° angle. The taxon can furthermore be diagnosed by a combination of characters, including the marked dorsal deflection of the dorsal margin of the skull at the beginning of the nasoantorbital fenestra, resulting in a concave rather than straight outline of the dorsal skull margin in this region in lateral view, and the pointed anterior process of the quadratojugal that separates the posterior ends of the jugal and the maxilla.

6. Description

MPEF-PV 11530 is preserved in a block (figure 2a) of a very thin and fine-grained pinkish-white to grey silicified mudstone, typical for the bone-bearing layers of the Queso Rallado locality, with one small partial counterpart of the cranial material (figure 2b). The elements that are preserved in the primary block include a partial cranium with two associated teeth, four dorsal vertebrae, and a metacarpal (either I, II or III). There are smaller bone shards and even a long bone shaft fragment interspersed throughout the remaining surface and interior (visible with CT scans) of the block; however, they are of indeterminate morphology.

6.1. Cranium

The right side of the cranium is preserved and has been split between the main slab and the counterslab during the discovery of the specimen, so that the former mainly contains the outer bone layer, with much of the bone substance preserved on the counterslab. The cranium is anteroposteriorly complete, but missing the dorsal skull roof, occiput, lateral and posterior walls (laterosphenoids-orbitosphenoids), and the floor of the endocranial cavity. It is laterally crushed (complicating the identification of individual elements) but includes the regions of the premaxilla, maxilla, jugal, ventral parts of the lacrimal and postorbital, fragments of the squamosal, partial quadratojugal and quadrate (figures 2 and 3). The cranium has an overall length of approx. 131.3 mm from premaxillary tip to the dorsal posterior end of the quadrate (table 1), with the rostrum anterior to the anterior margin of the orbit measuring 94.8 mm (therefore comprising about 72% of the skull, whereas the condition in derived



Of the main cranial openings, the ventral parts of the nasoantorbital fenestra, the orbit and the infratemporal fenestra are visible. The nares and anteorbital fenestra are visibly confluent to form a nasoantorbital fenestra, with a pointed anterior margin, and a ventral margin that is placed on a more dorsal level in the anterior half (probably corresponding to the original nares) than in the posterior half (probably corresponding to the original antorbital fenestra). The two portions of the ventral margin are separated by a marked step that is slightly undercut from the posterior side, and which we interpret as a vestigial ascending process of the maxilla (see below). Above this process, the openings are confluent and there is no indication of a dorsal extension of the ascending process contacting either the nasal or the lacrimal dorsally (cortical bone striations on the process also markedly run solely in the anteroposterior plane).

The orbit has straight anterior and posterior borders that diverge throughout the preserved height of the opening so that its anteroposterior width increases dorsally. The entire shape of the orbit cannot be established, due to the missing dorsal region. However, what is preserved does appear pyriform, with a rounded and approaching Vv-shaped ventral margin. The orbit measures 20.3 mm at the widest preserved anteroposterior point. The jugal-lacrima strut separating the orbit from the nasoantorbital fenestra is triangular, with a wide ventral base and its long axis almost perpendicular to the alveolar

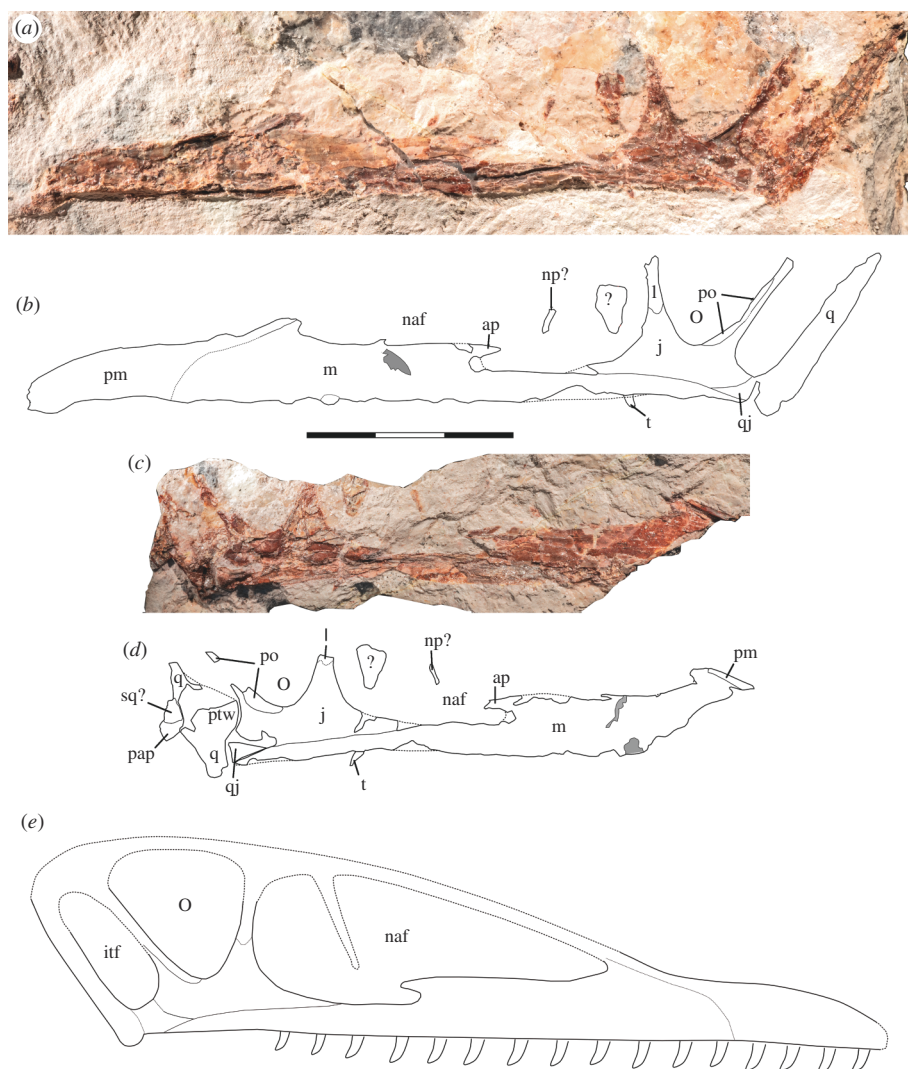


Figure 3. Holotype cranium of *Melkamter pateko* gen. et sp. nov., MPEF-PV 11530, in medial views. (a) pPhotograph of the main slab; (b) interpretative camera lucida drawing of the remains on the main slab; (c) photograph of the counterslab; (d) tentative interpretative camera lucida drawing of the remains on the counterslab; (e) reconstruction of the cranium (the size, number and arrangement of the teeth are conjectural). Scale bar is 3 cm. Abbreviations: ap = ascending process of the maxilla; itf = infratemporal fenestra; j = jugal; l = lacrimal; m = maxilla; naf = nasoantorbital fenestra; np? = possible fragment of the ventral process of the nasal; o = orbit; pap = paroccipital process; pm = premaxilla; po = postorbital; ptw = pterygoid wing of the quadrate; q = quadrate; qj = quadratojugal; sq? = possible squamosal fragment; t = possible last tooth.

border, as in darwinopterans (e.g. [6,66–68]) and basal pterodactyloids (e.g. [65]), but unlike the strongly anteriorly inclined strut in many non-monofenestratan pterosaurs, such as *Rhamphorhynchus* and *Scaphognathus* [65], *Dorygnathus* [69–71], *Campylognathoides* [15] or *Dimorphodon* [69]. The infratemporal fenestra was apparently high, but anteroposteriorly narrow and anteroventrally inclined so that its ventral end was placed below the orbit, as in many pterosaurs.

Although the crushed state of the specimen makes it difficult to discern any suturing (also further complicated by the sporadic distribution of cortical bone on either the part or counterpart of the fossil), it appears that the premaxilla is short, and is potentially fused to the maxilla where a slight dorsoventral crack occurs at about 20 mm from the anteriormost tip. A thin posterior dorsal process of the premaxilla seems to extend from here posterodorsally, flanking the dorsal margin of the maxilla and probably forming the dorsal margin of the nasoantorbital fenestra, as in other pterosaurs. There is no sign of a premaxillary crest, although one could have been more posteriorly placed along the dorsal margin of the skull than is preserved on the specimen.

The maxilla extends posteriorly from the contact with the premaxilla, contributing to the anterior and ventral margins of the nasoantorbital fenestra, until it is overlapped dorsally by the anterior

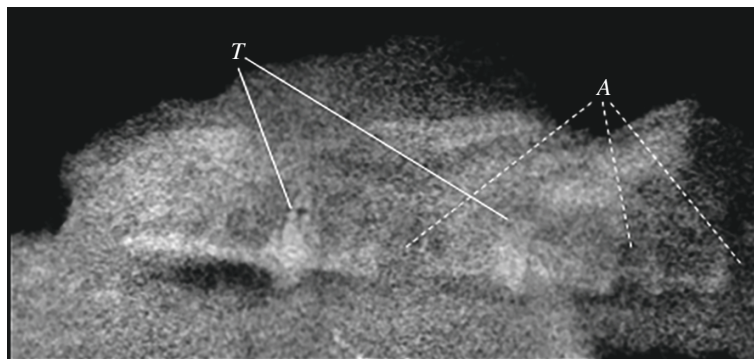


Figure 4. CT scan showing the position of two teeth (*Tt*) scanned on the slab inside the maxilla, with three additional empty alveolar (*Aa*) sockets.

Table 1. Measurements of MPEF-PV 11530, in millimetres.

preserved cranium length (anteroposteriorly)	131.3 mm
cranium length to jaw articulation	112.1 mm
preserved maximum cranium height	24.9 mm
rostrum to anterior nasoantorbital fenestra	40.8 mm
cranium height at anterior nasoantorbital fenestra	12.7 mm
nasoantorbital fenestra length	51.6 mm
preserved posterior nasoantorbital height	20.4 mm
cranium length to nasoantorbital fenestra posterior margin	93.6 mm
mediodistal width of dental alveolus	1.7
preserved maximum orbit length	18.0
preserved maximum orbit height	15.8
infratemporal fenestra length	6.2
manual metacarpal length	29.2
manual metacarpal mid-width	1.3
dorsal vertebra centrum length	9.7
dorsal vertebra neural spine length	5.8

process of the jugal. The maxilla continues below the jugal to at least the mid-length of the orbit. The anterior half of the maxillary body below the nasoantorbital fenestra is approximately twice as high dorsoventrally (*ca.* 8 mm) than the posterior half (maximally 4 mm). In between these two sections, a small incision into the posterior end of the anterior half is present within the nasoantorbital opening. We interpret this incision as marking the posterior end of a vestigial ascending process of the maxilla, which is thus almost entirely posteriorly directed and does not contact a ventral process of the nasal or lacrimal (figures 3 and 5*b*). The dorsal margin of this process is partially preserved in the counterslab, and curves downwards in its posterior part, resulting in a very slender termination of the process (figure 5).

One tooth is visibly well-preserved on the surface of the block (figure 2*b*) as well as one additional fragmentary tooth, both in close association to the cranium, and although no teeth are visibly attached to the rostrum, CT data (figures 2 and 4) show that several alveoli (at least 5 per side) are indeed present and regularly spaced throughout the maxillopremaxillary region, with at least two partial teeth present within their individual alveolar sockets. Several empty sockets are also visible, but image quality precludes discerning how far anteriorly or posteriorly this toothrow extends. There is a small, posteroventrally inclined splinter in the posterior part of the maxilla that might represent a remnant of a tooth; if correctly identified, the tooth row would at least extend to the posterior margin of the nasoantorbital fenestra. Individual alveoli are widely spaced, with the distance between alveoli equalling almost two tooth widths in the anterior part of the maxilla. The completely preserved tooth (figure 5*c*) is apicobasally short (4.3 mm), and anteroposteriorly thin (1.7 mm at the widest point of the

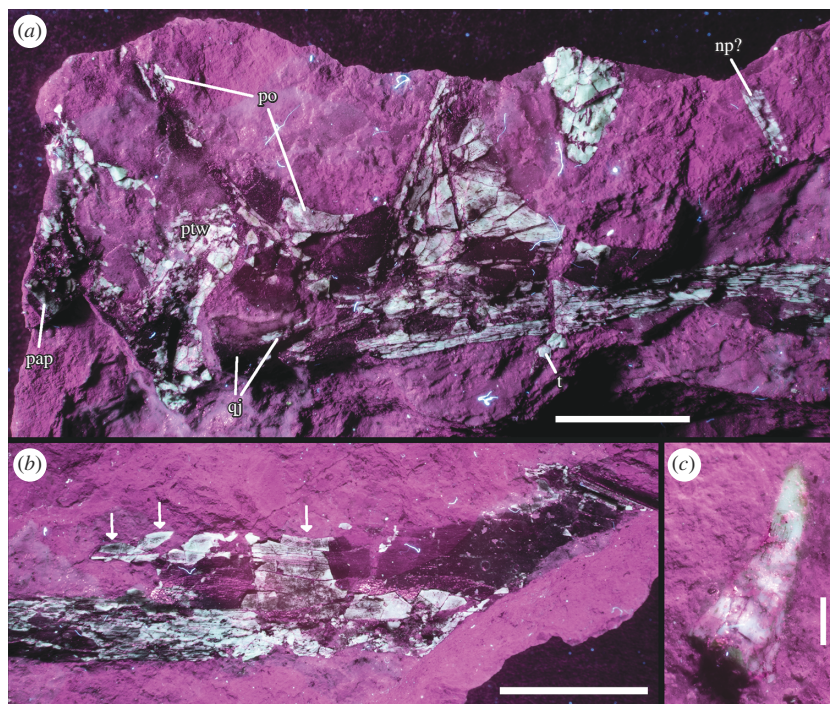


Figure 5. Details of the holotype cranium of *Melkamter pateko* gen. et sp. nov., MPEF-PV 11530, under UV light. (a) pPosterior part of cranium as preserved on the counterslab; (b) anterior part of the maxilla as preserved on the counterslab; (c) isolated tooth, preserved on the main slab. Abbreviations as in figure 3. Arrows in (b) point to preserved original margins of the base and the distal part of the ascending process of the maxilla. Scale bars, are 1 cm (a, b) 1 cm and 1 mm (c) 1 mm.

base), with the shape of a curved cone, similar to that of basal pterodactyls such as *Germanodactylus* sp. and *Pterodactylus* sp. The tooth also exhibits a gradual apical taper with a gentle curvature, such that the tip is at an about a 10° offset to its base.

The triradiate jugal tapers to a point anteriorly and contacts the maxilla anteriorly with a seemingly elongate process, together forming the flat ventral margin of the nasoantorbital fenestra (figure 3). Although the exact contact of the anteroventral jugal process with the maxilla cannot be confidently distinguished, it can be estimated to form approx. 13 mm of the posterior ventral margin of the nasoantorbital fenestra. The lacrimal process of the jugal rises in an almost perpendicular curve in respect to its ventral margin. Both this ascending process and the posterior postorbital ramus taper dorsally, reaching about the halfway point of the preserved orbit. The lacrimal process is considerably more massive than the postorbital process and contacts the ventral ramus of the lacrimal at about the mid-height of the orbit, or slightly lower. Although the suture is poorly preserved, the ventral end of the lacrimal seems to slot into a notch in the dorsal end of the jugal. The postorbital process is slender and reaches approximately as far dorsally as the lacrimal process (figure 5). Anteriorly, it is overlapped by a rather massive ventral process of the postorbital, which forms the entire posterior margin of the orbit and reaches the mid-length of this opening ventrally. The angle formed by the lacrimal and postorbital processes of the jugal is set at about 55°. A short and dorsoventrally broad posterior process of the jugal is also present. Only the anterior end of the quadrate is preserved. It is triangular in outline, tapering anteriorly, and inserts in between the ventral margin of the posterior end of the jugal and the dorsal margin of the posterior end of the maxilla, as in *Cynorhamphus* [72].

The quadrate appears long and broad, inclined posterodorsally backwards at about 126° from the plane of the palate. It forms the posterior boundary of the infratemporal fenestra. On its ventral-most point, there is a small, bulbous articular protuberance for articulation with the mandible. The large, anteriorly rounded pterygoid wing of the quadrate is partially preserved. It is offset from the ventral end of the quadrate and rapidly expands anteriorly in its ventral part, whereas the dorsal end grades more gradually into the quadrate shaft. On the counterslab, the end of the paroccipital process is preserved, and anterodorsal to it is a strongly eroded piece of bone that most probably represents a remnant of the squamosal.

Four dorsal vertebrae are preserved in the block (two isolated, and two in close articulation with each other) (figure 6a–c). Of the two isolated vertebrae preserved, one is visible in lateral view (figure

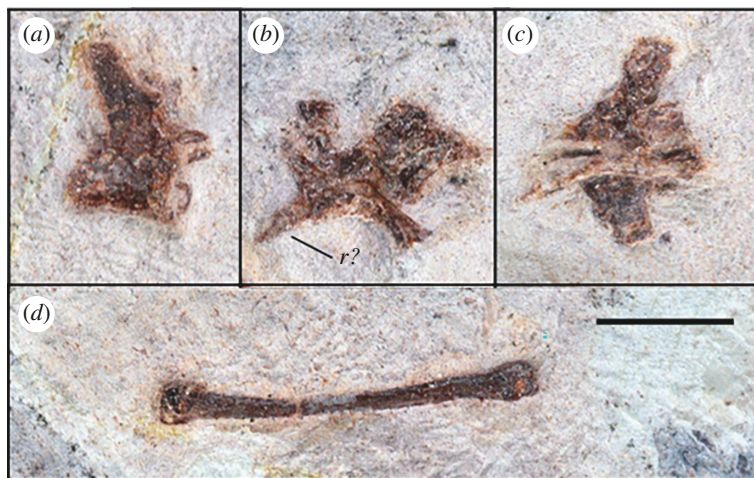


Figure 6. Details of MPEF-PV 11530 postcranial material: (a–c) dorsal vertebrae and (d) manual metacarpal. Scale bar is 1 cm. Abbreviations: *r* = rib.

6a) and one in dorsal view (figure 6c), with the articulated vertebrae in anterolateral view (figure 6b). From these perspectives, the shapes of the centra are procoelous, and in lateral view, there is a slight dorsoventral constriction of each centrum, giving a spool-shaped profile. The transverse processes have an anteroposteriorly broad base until the capitular facet is reached, from which point they project dorsolaterally as they taper gently to a rounded tip (figure 6a). The location of the capitular facet (about halfway along the length of the transverse process) also contributes anteriorly to the lateral margin of the prezygapophysis, similar to darwinopterans [9]. Due to the taphonomic state of the vertebrae, it is not possible to distinguish the presence of any foramina. The neural spines of the two articulated dorsals contact each other completely, with only a very faint line visibly demarcating them. These two dorsals also potentially preserve an articulated fragmentary dorsal rib, although this is difficult to distinguish in their fractured state.

One metacarpal is completely preserved (either metacarpal I, II or III). A shaft fragment (potentially another metacarpal I–III) and another large indeterminate bone shard are also preserved on the surface of the block. However, all are too eroded to glean any further information.

6.2. Systematic palaeontology

PTEROSAURIA Owen, 1842 [59]

PTERODACTYLOIDEA Plieninger, 1901 [73]

CTENOCHASMATIDAE(?) *indet.* Nopsca, 1928 [74] *sensu* Unwin, 2003 [31]

In addition to the above-mentioned specimen, a separate block containing an isolated tooth was also recovered from the Queso Rallado locality of the Cañadón Asfalto Formation, which closely resembles the teeth of ctenochasmatids (figure 7). The sediment comprising the block is different in colour and texture from the above-mentioned specimen, likely indicating that it originated from a different horizon. The tooth is in good condition overall, preserving most of the crown, and missing only the apical-most tip (although a natural mould in the surrounding sediment retains its overall original shape). The base of the tooth appears to have been broken (likely near the crown–root boundary), perhaps during feeding, but the lack of erosion over the entire tooth surface indicates that it was not likely to be much transported after its dissociation from the rostrum. The tooth is remarkably elongated, slightly recurved, and measuring 47 mm from base to tip, 1.5 mm wide at its base and gradually tapering to 0.5 mm wide at its apical tip. At the base, it is lenticular in cross-section, but becomes more circular in cross-section as it approaches the apex, as in most ctenochasmatids, and similar to the morphology of the anterior teeth (from the third to the sixth–seventh) of *Pterodaustro guinazui* [24]. There is an ombre-like colour change from base to tip, varying from grey to beige, which is also indicative of the dentine-to-enamel change, with the enamel thickening apically (the



Figure 7. Isolated ctenochasmatid(?) tooth MPEF-PV 2549[2012], also from the Queso Rallado locality. Scale bar is 1 cm.

lower grey 30 mm of the tooth representing exposed dentine as it is less shiny than the more apical beige enamelled region). The enamel is completely smooth and lacks any ornamentation. Due to the proportion of dentine-to-enamel present, it is likely that the tooth is from the anteriormost region of a ctenochasmatid rostrum (as anterior teeth are also subject to more breakage during feeding) [75,76].

6.3. Phylogenetic analysis

The analysis of the matrix based on Fernandes *et al.* [55] under equal weights resulted in the recovery of 12 equally parsimonious trees with a score of 1388.014 (figure 8). The results are generally comparable to those published by Andres [56], but show less resolution, with some polytomies being present. *Melkamter* is found in a polytomy with *Sordes* just outside the Darwinoptera–Pterodactyloidea clade in this analysis. Interestingly, *Allkaruen* is still found in a polytomy with species of *Dimorphodon* in the Dimorphodontia, as in the original analysis of Andres [56], despite the revised scorings for this taxon. Constraining *Allkaruen* into the clade including *Sordes* and monofenestratans (as found by [5,13]) requires three additional steps (score of 1391.221) and finds this taxon within derived pterodactyloids as a member of the Istiodactylinae; given that the holotype of *Allkaruen* mainly consists of a complete, three-dimensionally preserved braincase [13], the rather limited sampling of braincase characters might account for these vastly differing results.

using the Fernandes *et al.* [55] matrix (simplified in Adobe Illustrator).

The equal weights analysis using the matrix based on Martin-Silverstone *et al.* [5] recovered 28 560 equally parsimonious trees with a length of 556 steps (figure 9). The strict consensus of these trees largely confirms to the results of Martin-Silverstone *et al.* [5], but shows both *Melkamter* and *Allkaruen* in a polytomy with darwinopterans at the base of Monofenestrata. Reduced consensus methods identify *Allkaruen* as a problematic taxon in this part of the tree, the *a posteriori* deletion of which results in *Melkamter* being found as the earliest branching monofenestratan, followed by a monophyletic Darwinoptera and pterodactyloids. *Allkaruen* can take multiple positions within this phylogenetic hypothesis, either below or just above *Melkamter*, as a sister taxon to the latter, as a darwinopteran or as the earliest branching pterodactyloid. The implied weights analysis of this matrix recovered 51 trees of a score of 22.36738 and finds *Melkamter* and *Allkaruen* in a polytomy at the base of Monofenestrata.

7. Discussion

7.1. Phylogenetic position and evolutionary implications

The phylogenetic analyses based on both different datasets agree in placing the new taxon described here just outside the clade encompassing darwinopterans and pterodactyloids (for the [5] phylogeny) or darwinopterans and pterodactyliiformes (for the [55] phylogeny). In the implied weights analysis of the [55] matrix, *Melkamter* is in a polytomy with *Sordes*, as oldest and earliest branching monofenestratan, followed by the Darwinoptera and Pterodactyliiformes (*sensu* [56]). As the Monofenestrata are an apomorphy defined clade, characterized by the presence of a confluent nasoantorbital fenestra [56], the

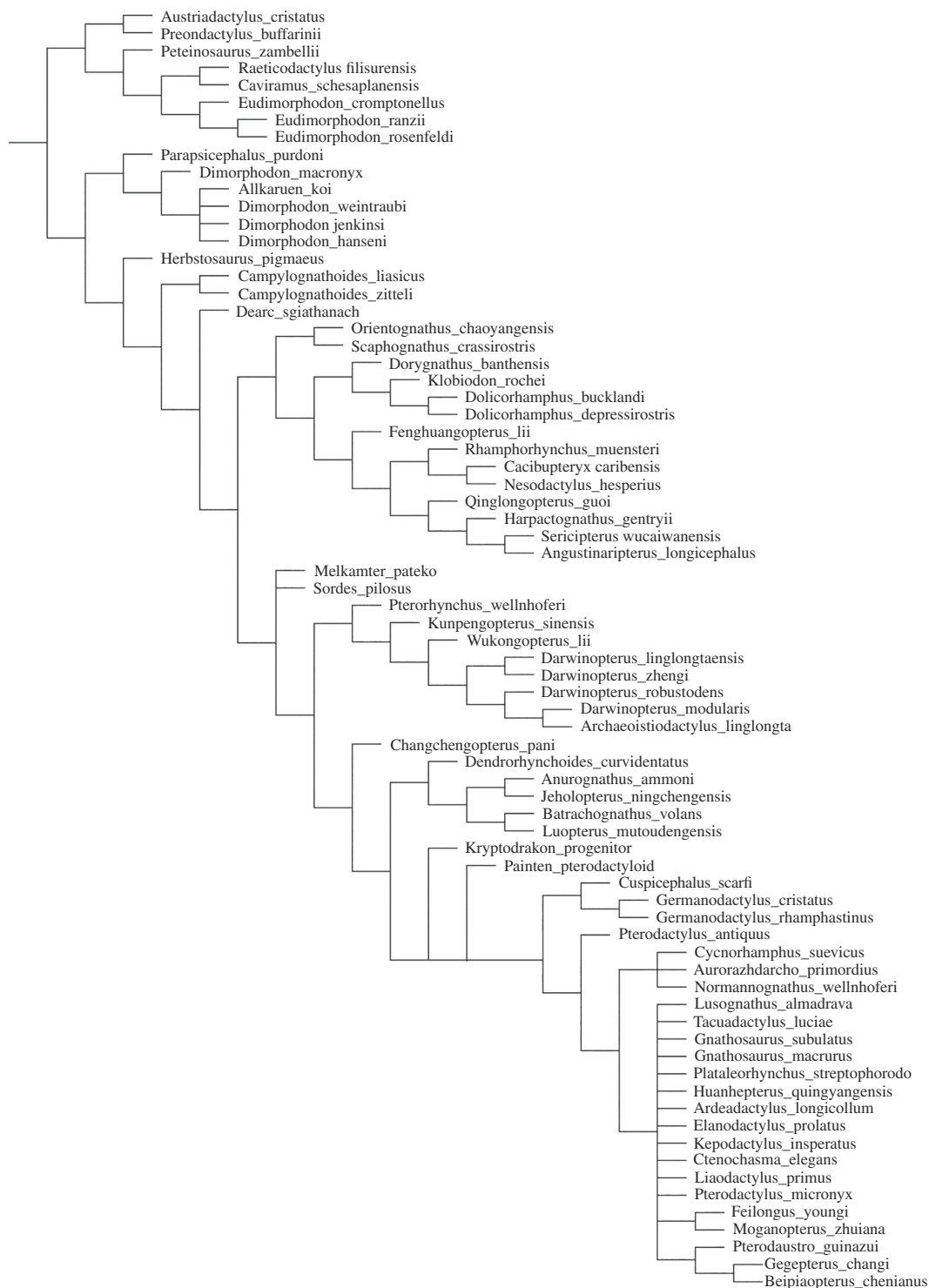


Figure 8. The relationship of *Melkamter pateko* to the Pterosauria, using the Fernandes *et al.* [55] matrix (simplified in Adobe Illustrator).

presence of this trait in the material described here and its phylogenetic position allows its reference to this clade. The presence of *Melkamter* in the Cañadón Asfalto Formation therefore marks the earliest worldwide occurrence (late Early Jurassic, Toarcian [28,40]) of a monofenestratan pterosaur, predating the currently oldest member of that clade [5] by at least 8 and probably 10 million years. However, the clade had seemingly achieved a wider distribution by at least the Middle Jurassic [5], and a probably worldwide distribution by the early Late Jurassic.

Melkamter is the first and only non-pterodactyloid monofenestratan from Gondwana. However, direct comparisons of *Melkamter pateko* with other non-pterodactyloid monofenestratans (outside of



Figure 9. The relationship of *Melkamter pateko* to the Pterosauria, using the Martin-Silverstone *et al.* [5] matrix (reduced consensus; strict consensus in electronic supplementary material).

the darwinopterans) is complicated for lack of their overlapping anatomical elements. In particular in comparison with its fellow Argentine taxon, *Allkaruen koi* from the same formation, it therefore cannot be entirely excluded that they are the same taxon as the two taxa do not have any overlapping material in common. However, in addition to the results of the phylogenetic analyses of the [55] matrix, where these two taxa come out in widely different positions (and in which forcing together *Melkamter* and *Allkaruen* requires five additional steps), the only morphological evidence that is comparable, the relative size and shape of the alveoli, also contradicts this, as the alveoli of the similar-sized holotype of *Allkaruen* seem to be relatively larger and more mediolaterally compressed than those of *Melkamter*.

Regarding comparison with darwinopterans, since the time of its initial description, *Cuspicephalus scarfi* Martill & Etches (2012) [77] (figure 10c) has been further prepared from its opposite side (which is

better preserved), allowing for a more direct observation of its morphology and more direct comparison with *Melkamter pateko* and other darwinopterans (figure 10). Although the cranium of *Cuspicephalus* is about twice the length of that of *Melkamter*, they both exhibit broad ascending processes of their jugals, as do *Kunpengopterus sinensis* and *Darwinopterus modularis* (but unlike *Darwinopterus linglongensis*). However, although some phylogenies do indeed regard it as a darwinopteran [77,78,5], one phylogenetic analysis herein recovers *Cuspicephalus* as a germanodactylid [55], instead of its initial assignment as a non-pterodactylid monofenestratans [77].

The overall shape of the cranium in *Melkamter pateko* suggests a high skull, as in *Darwinopterus linglongtaensis* Wang et al. (2010), [79], which is higher than that of both *Kunpengopterus sinensis* [79] and *Darwinopterus modularis* [79]. *Kunpengopterus* lacks a premaxillary crest (tentatively matching the condition of *Melkamter*), making it unlike other darwinopterans. However, the quadrate of *Kunpengopterus* is inclined more dramatically than in the specimen herein (150°, as opposed to about 126° in *Melkamter*). The inclination found in *Dimorphodon* is 95° [80,81], in *Parapsicephalus* it is between 115° and 130°, *Eudimorphodon* and *Scaphognathus* are at 120° [82,83], *Dorygnathus* and *Campylognathoides* are between 120° and 130° [70,71], *Rhamphorhynchus* is at 130°–150° [61,65,84] and *Angustinaripterus* is at 140° [85]. Among darwinopterans the angle varies from about 130° to 132° in *Darwinopterus linglongtaensis* to 142° in *Kunpengopterus*, and 140° in *Cuspicephalus* [77]. Germanodactylids are further set at about 148°, with more derived pterodactylids having even larger angles of inclination. This places *Melkamter* as having a more acute angle than the darwinopterans (figure 10), with a value closer to those found in the more basal scaphognathines and campylognathoidids than in the more derived pterodactylids.

Although potentially ontogenetically variable, the angle of the orbit (formed by the lacrimal and posterior processes of the jugal, and measured from photographs of each specimen) in *Cuspicephalus* is set at 45°, *Parapsicephalus* at 45°, *Angustinaripterus* at 46°, *Tupandactylus* at 45°, *Dimorphodon* at 47°, *Darwinopterus modularis* at 60°, *Germanodactylus cristatus* at 63°, *Pteranodon* at 65°, *Germanodactylus rhamphastinus* at 70°, *Dorygnathus* at 72°–96°, *Pterodactylus micronyx* (the neotype) at 75°, *Cynorhamphus* at 76°, *Campylognathoides* at 77°, *Eudimorphodon* at 80°, *Ctenochasma* at 80°–85°, *Scaphognathus* at 80°–100°, *Rhamphorhynchus* at 82°, and 90° in *Pterodactylus antiquus* (the holotype) [65,70–72,84–90]. *Melkamter* expresses an angle of about 55°, which places it with a value closer to those found between *Dimorphodon* and *Darwinopterus*.

Darwinopterans usually exhibit pterodactylid-like elongated crania with confluent nasoantorbital fenestrae, free nasal processes, inclined quadrates and short peg-like teeth [91,6,79,92–94], all of which are exhibited by *Melkamter*. Despite their traditionally held modular evolution, however, it has also been recently argued that darwinopterans should no longer be considered a directly transitional group between basal non-pterodactylids and the Pterodactyloidea, but rather a sister group to the Pterodactyloidea, along with the scaphognathines and rhamphorhynchines [5]. One significant autapomorphy seen in *Melkamter* holds merit in making this distinction: that of a vestigial ascending process of the maxilla, which is absent in all other known monofenestratans, and could potentially show the evolutionary pathway to the pterodactylids losing this feature completely.

Concerning the tooth MPEV PV 2549, a secure identification of such an isolated element is, of course, difficult. The extreme elongation of this tooth is remarkable; such elongate teeth are unknown from any other terrestrial Mesozoic vertebrate clade, but elongate, recurved and pointed teeth are quite frequently found in pterosaurs [(see [4,62]). A further argument for a pterosaur identification of this tooth is the unusual distribution of enamel: an apical enamel cap and dentine base to the crown (with a distinct enamel–dentine junction demarcating them), which is similarly found in other pterosaur clades (e.g. [4,75]). Inclusion of the tooth in the phylogenetic analyses above was attempted, but results were inconclusive for lack of characters. However, within pterosaurs, the tooth is most similar to the teeth of ctenochasmatids, which have strongly very elongate, slender teeth with a marked curvature in at least the mesial teeth (see e.g. [87]). If the presence of a (probably early branching) ctenochasmatid from the Cañadón Asfalto Formation can be confirmed, this would considerably extend the fossil record of pterodactylids and place the origin of this clade firmly in the Early Jurassic. The tooth is unusually large for known ctenochasmatids, being approximately double the length of the mesial teeth of a skull of *Gnathosaurus* from the Tithonian Altmühltal Formation of Eichstätt, Germany [87] and even larger if compared to known large specimens of ctenochasmatids (e.g. [95]) but the discovery of the very large jaw of *Lusognathus* demonstrates that ctenochasmatids could reach large sizes already in the Jurassic (i.e. the estimated 3.6 m wingspan of *Lusognathus almadrava* [55]). Therefore, the tooth is here tentatively assigned to the Ctenochasmatidae, thus extending the stratigraphic range of this clade by at least 10–15 million years [92]. As ctenochasmatids are well nested within

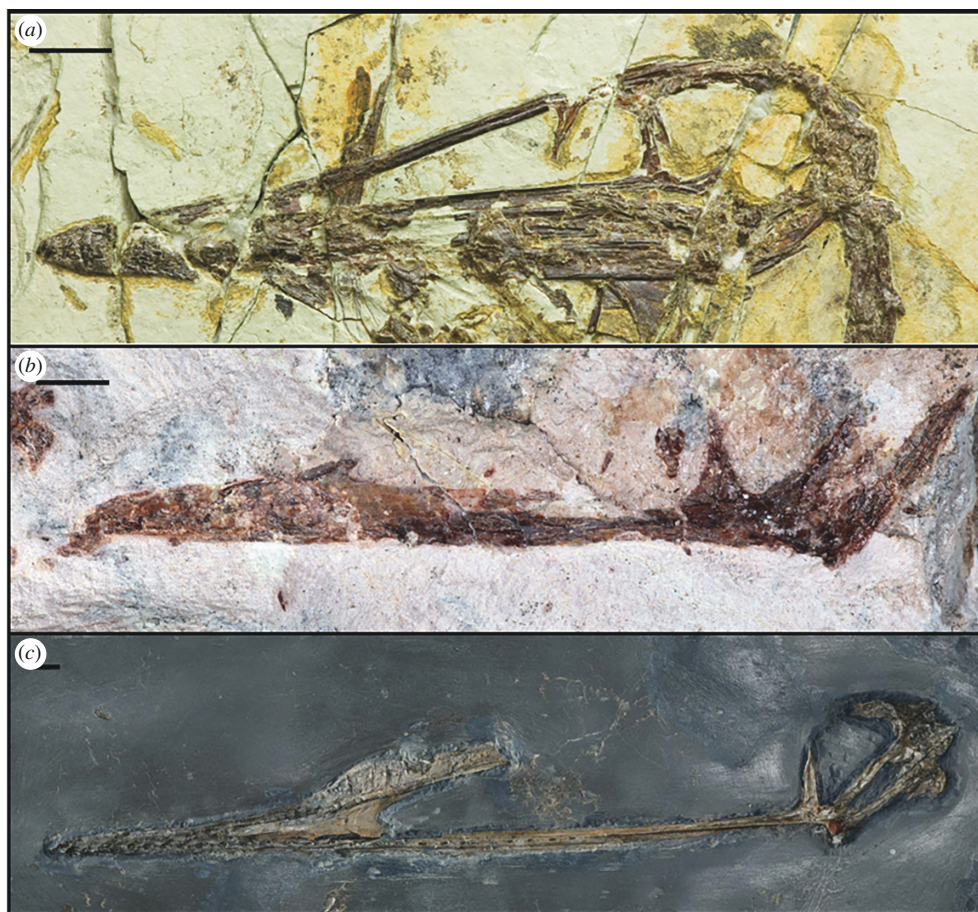


Figure 10. Comparison of (a) *Darwinopterus linglongensis* (IVPP V16049; mirror-imaged for comparison), (b) *Melkamter pateko*, and the newly- prepared left side of (c) *Cuspicephalus scarfi*. Scale bars are 1 cm.

Pterodactyloidea, this would furthermore extend the entire clade and its early diversification into the Early Jurassic. However, as other, more basal pterosaurs also show elongate and curved teeth, including the rhamphorhynchids (e.g. [65,70,71]), it cannot be excluded that this tooth represents an independent acquisition of such extremely elongate teeth, allowing for the possibility that it could belong to some other novel taxon entirely. Nevertheless, the tooth represents a taxon different from both *Allkaruen* and *Melkamter*, thus further increasing pterosaur diversity in the Cañadón Asfalto Formation.

7.2. Dentition and ecological implications

Great variability is shown in the basal monofenestratan dentition. *Propterodactylus frankerlae* Spindler *et al.* (2024) [16] has pointed, conical long teeth with large interdental spaces and rostrolaterally directed fangs in the rostral jaw area [15,16], *Darwinopterus modularis* exhibits spike-like teeth [3], *Darwinopterus linglongtaensis* and *Kunpengopterus sinensis* have short blunted cone-shaped teeth, *Wukongopterus lüi* has cone-shaped and very pointed teeth [79], and *Darwinopterus robustadens* exhibits relatively stout teeth [3,67]. This variation in dental morphology has been interpreted as evidence of niche partitioning [3,18,67,79] and the feeding on different prey items, although all these taxa are overall generally regarded as being insectivorous or piscivorous [18,94]. Based on the short, stout, conical tooth morphology, darwinopterans were probably insectivores [18,94], but the high tooth count of *Cuspicephalus scarfi* could also potentially indicate piscivory [77,91]. This is all in keeping with the relative abundance of arthropods present in some concurrent deposits (e.g. [18]), and fish in others (e.g. the Tiaojishan Formation and Daohugou beds of [79]). The dental morphology and regular tooth spacing of the *Melkamter* appear to be of the insectivorous morphotype [94], warranting more similarity with wukongopterids, which also exhibit interalveolar spacing that is greater than their tooth lengths [22], characteristics which are shared with the specimen herein. Whereas many pterosaurs from the ‘classic’ marine Lagerstätten (e.g. the Rhamphorhynchidae) show adaptations to a piscivorous diet



Figure 11. Artistic reconstruction of *Melkamter pateko* by Pedro Andrade.

(see [62,94]), this concentration of insectivorous forms in the early branching monofenestratans might support the suggestion of Andres *et al.* [1] that the origin of pterodactyloids might be found in truly terrestrial rather than nearshore or insular environments. This is especially the case in the phylogenetic hypothesis based on the Andres [56] and Fernandes *et al.* [55] datasets, in which the Anurognathidae, for which there is the strongest evidence and consensus for an insectivorous diet [94], represent the immediate outgroup to Pterodactyloidea. Given the otherwise expressed dietary plasticity in pterosaurs (see [94,96]), such a preference for terrestrial prey in non-pterodactyloid monofenestratans could be unexpected if these animals lived in nearshore environments or on islands in a lagoonal setting.

Ecological requirements (such as prey preferences) do affect the dispersion of animals, even beyond their ability to fly [97]. However, considering that the prey of insectivorous animals also fly (albeit with a likely smaller range), this could potentially indicate that insectivorous monofenestratans could have a wide dispersion (even across wider geographical barriers than those feeding solely on lacustrine fish, for example), setting different natural geospatial limits on the ecological niches that they occupied. Thus, in a still Pangean world during the Early and Middle Jurassic, a largely insectivorous diet might have represented an important adaptation in the success of basal monofenestratans and their descendants, the pterodactyloids.

8. Conclusion

It has long been suspected that pterodactyloids were already present by the end of the Early Jurassic [14,21], and that pterosaurs had already reached relatively high levels of taxonomic and morphological diversity by the Middle Jurassic [5], although the dearth of available fossil material has made these claims difficult to concretely establish. *Melkamter pateko* (figure 11), from the latest Early Jurassic of Chubut Province, represents the so far most conclusive evidence for the presence of Monofenestrata during the late Early Jurassic, while also contributing to their morphological diversity with the novel traits expressed in this new taxon. Furthermore, if confirmed by future finds, the possible presence of a ctenochasmatid, currently indicated by a single tooth, would not only place the origin of pterodactyloids into the Early Jurassic, but even indicate that their initial diversification already happened during that time. Although the Lagerstätten of the Northern Hemisphere have traditionally dominated in our understanding of the diversity and dispersion of pterosaurs over time, it is clear now that Gondwana also held a high phylogenetic diversity of Early Jurassic pterosaurs, with the Cañadón Asfalto Formation alone now exhibiting evidence for at least three distinct taxa. This further highlights our still-lacking knowledge of Jurassic pterosaur faunas from Gondwana, and it is evident that, pending more field sampling and pterosaur fossil recovery, the inherent potential is present for the Southern Hemisphere to perhaps one day match the abundance of the Northern Hemisphere.

Ethics. This work did not require ethical approval from a human subject or animal welfare committee.

Data accessibility. All phylogenetic matrices used are available in the electronic supplementary material [98], as well as at <https://morphobank.org/permalink/?P4589>. CT scan data are made available at <https://www.morphosource.org/concern/media/000649886?locale=en>.

Declaration of AI use. We have not used AI-assisted technologies in creating this article.

Authors' contributions. A.E.F.: conceptualization, data curation, formal analysis, investigation, methodology, software, visualization, writing—original draft, writing—review and editing; D.P.: funding acquisition, methodology, resources, software, supervision, validation, writing—review and editing; O.W.M.R.: conceptualization, formal analysis, funding acquisition, investigation, project administration, resources, software, supervision, validation, visualization, writing—review and editing.

All authors gave final approval for publication and agreed to be held accountable for the work performed therein.

Conflict of interest declaration. We declare we have no competing interests.

Funding. A.E.F. is supported by funding from DFG grant number RA 1012/29. Fieldwork was supported by ANPCyT PICT 2014-1288 and 2019-03834 (to D.P.) and NSF grants DEB 0946430 and DEB1068089 (to Guillermo Rougier).

Acknowledgements. These specimens were found as part of the ongoing quarrying project of the Queso Rallado locality that has been led by Guillermo Rougier throughout the last 20 years. We thank Guillermo and the successive crews for this effort. Many thanks go to José Carballido, Pablo Puerta, Ariel Aresti, Mariano Caffa, and Vanessa Béland for their invaluable research and pterosaur field assistance, and to the entire staff of the MEF. Heartfelt thanks are extended to Calin Suteu for his photographic expertise, and to Victor Beccari for his CT segmentation and UV photography assistance. Thank you to Mike Day at the NHM London and Steve Etches of the Etches Collection for granting access to specimens. Thank you to Dr Xu Xing and Dr Shunxing Jiang for their kindness in providing information on the Chinese taxa included in the work. We also thank Brian Andres for his critical comments on the material, and significant insights into the manuscript. We are also grateful to the reviewers for their constructive feedback, which improved this work. This work was supported by the Deutsche Forschungsgemeinschaft (DFG) under project RA 1012/29. Field work was made possible by the authorities of the Secretaría de Cultura de la Provincia del Chubut, and supported by the Fundación Egidio Feruglio.

References

- Andres B, Clark J, Xu X. 2014 The earliest pterodactyloid and the origin of the group. *Curr. Biol.* **24**, 1011–1016. (doi:10.1016/j.cub.2014.03.030)
- Yu Y, Zhang C, Xu X. 2023 Complex macroevolution of pterosaurs. *Curr. Biol.* **33**, 770–779. (doi:10.1016/j.cub.2023.01.007)
- Lü J, Unwin DM, Jin X, Liu Y, Ji Q. 2009 Evidence for modular evolution in a long-tailed pterosaur with a pterodactyloid skull. *Proc. R. Soc. B* **277**, 383–389. (doi:10.1098/rspb.2009.1603)
- Witton MP. 2013 *Pterosaurs: natural history, evolution, anatomy*. Princeton, NJ: Princeton University Press.
- Martin-Silverstone EM, Unwin DM, Cuff AR, Brown EE, Allington-Jones L, Barrett PM. 2024 A new pterosaur from the Middle Jurassic of Skye, Scotland and the early diversification of flying reptiles. *J. Vertebr. Paleontol.* **43**, e2298741. (doi:10.1080/02724634.2023.2298741)
- Lü J, Unwin DM, Jin X, Liu Y, Ji Q. 2010 Evidence for modular evolution in a long-tailed pterosaur with a pterodactyloid skull. *Proc. R. Soc. B* **277**, 383–389. (doi:10.1098/rspb.2009.1603)
- Butler RJ, Benson RBJ, Barrett PM. 2013 Pterosaur diversity: untangling the influence of sampling biases, Lagerstätten, and genuine biodiversity signals. *Palaeogeogr. Palaeoclimatol. Palaeoecol.* **372**, 78–87. (doi:10.1016/j.palaeo.2012.08.012)
- Dean CD, Mannion PD, Butler RJ. 2016 Preservational bias controls the fossil record of pterosaurs. *Palaeontology* **59**, 225–247. (doi:10.1111/pala.12225)
- Pentland AH, Poropat SF. 2023 A review of the Jurassic and Cretaceous Gondwanan pterosaur record. *Gondwana Res.* **119**, 341–383. (doi:10.1016/j.gr.2023.03.005)
- Martínez RN, Andres B, Apaldetti C, Cerda IA. 2022 The dawn of the flying reptiles: first Triassic record in the southern hemisphere. *Pap. Palaeontol.* **8**, e1424. (doi:10.1002/spp2.1424)
- Codorniu L, Gianchini FA. 2016 The flying reptiles from Argentina: an overview. In *Historia evolutiva y paleobiogeográfica de los vertebrados de América del Sur* (eds FL Agnolin, GL Lio, FB Egli, NR Chimento, FE Novas). Buenos Aires, Argentina: Contribuciones del Macn.
- Barrett PM, Butler RJ, Edwards NP, Milner AR. 2008 Pterosaur distribution in time and space: an atlas. *Zitteliana* **B28**, 61–107.
- Codorniu L, Paulina Carabajal A, Pol D, Unwin D, Rahut OWM. 2016 A Jurassic pterosaur from Patagonia and the origin of the pterodactyloid neurocranium. *PeerJ* **4**, e2311. (doi:10.7717/peerj.2311)
- O'Sullivan M, Martill D. 2018 Pterosauria of the great oolite group (Middle Jurassic, Bathonian) of Oxfordshire and Gloucestershire, England. *Acta Palaeontol. Pol.* **63**. (doi:10.4202/app.00490.2018)
- Tischlinger H, Frey E. 2013 A new pterosaur with mosaic characters of basal and pterodactyloid pterosauria from the Upper Kimmeridgian of Painten (Upper Palatinate, Germany). *Archaeopteryx* **31**, 1–13.
- Spindler F. 2024 A pterosaurian connecting link from the late Jurassic of Germany. *Palaeontol. Electron.* **27**, a35. (doi:10.26879/1366)
- Rahut OWM. 2012 Ein 'rhamphodactylus' aus der mörsheim-formation von mühlheim. In *Jahresbericht 2011 und mitteilungen der freunde der bayerischen staatssammlung für paläontologie und historische geologie münchen e.v.*, pp. 69–74.
- Zhou X *et al.* 2021 A new darwinopteran pterosaur reveals arborealism and an opposed thumb. *Curr. Biol.* **31**, 2429–2436. (doi:10.1016/j.cub.2021.03.030)

19. Wang X, Kellner AWA, Jiang S, Meng X. 2009 An unusual long-tailed pterosaur with elongated neck from western Liaoning of China. *An. Acad. Bras. Cienc.* **81**, 793–812. (doi:10.1590/s0001-37652009000400016)
20. Unwin DM, Lü J, Bakhurina NN. 2000 On the systematic and stratigraphic significance of pterosaurs from the Lower Cretaceous Yixian Formation (Jehol Group) of Liaoning, China. *Mitt. Mus. Nat.kd. Berl. Geowiss. Reihe* **3**, 181–206. (doi:10.1002/mmng.4860030109)
21. Unwin DM. 1996 The fossil record of middle jurassic pterosaurs. In *The continental jurassic* 291–304, vol. 60 (ed. M Morales). Flagstaff, AZ: Museum of Northern Arizona Bulletin.
22. Witton MP. 2015 Were early pterosaurs inept terrestrial locomotors? *PeerJ* **3**, e1018. (doi:10.7717/peerj.1018)
23. Rauhut OWM, López-Arbarelló A. 2008 Archosaur evolution during the Jurassic: a southern perspective. *Rev. Asoc. Geol. Arg.* **63**, 557–585.
24. Codorniu L, Chiappe LM, Cid FD. 2013 First occurrence of stomach stones in pterosaurs. *J. Vertebr. Paleontol.* **33**, 647–654. (doi:10.1080/02724634.2013.731335)
25. Rauhut OWM, Martin T, Ortiz-Jaureguizar E, Puerta P. 2002 A Jurassic mammal from South America. *Nature* **416**, 165–168. (doi:10.1038/416165a)
26. Unwin DM, Rauhut OWM, Haluza A. 2004 The first rhamphorynchoid from South America and the early history of pterosaurs. In *74th Annual Meeting of the Paleontologische Gesellschaft*, pp. 235–237.
27. Codorniu L, Gasparini Z. 2007 Pterosauria. In *Patagonian mesozoic reptiles* (eds Z Gasparini, L Salgado, RA Coria), pp. 143–166. Bloomington, IN: Indiana University Press.
28. Pol D, Ramezani J, Gomez K, Carballido JL, Carabajal AP, Rauhut OWM, Escapa IH, Cúneo NR. 2020 Extinction of herbivorous dinosaurs linked to Early Jurassic global warming event. *Proc. R. Soc. B* **287**, 20202310. (doi:10.1098/rspb.2020.2310)
29. Goldfuß GA. 1831 Beiträge zur Kenntnis verschiedener Reptilien der Vorwelt. *Nova acta Acad. caes. Leop.-Carol. germ. naturae curios.* **15**, 61–128.
30. Lawson DA. 1975 Could pterosaurs fly. *Science* **188**, 676–678. (doi:10.1126/science.188.4189.676-b)
31. Unwin DM. 2003 On the phylogeny and evolutionary history of pterosaurs. *Geol. Soc. Lond. Spec. Publ.* **217**, 139–190. (doi:10.1144/GSL.SP.2003.217.01.11)
32. Codorniu L, Rauhut OWM, Pol D. 2010 Osteological features of Middle Jurassic pterosaurs from Patagonia (Argentina). *Acta Geosci. Sin.* **31**, 12–13.
33. Casamiquela RM. 1975 *Herbstosaurus pigmaeus* (Coeluria, Compsognathidae) n. gen. n. sp. del Jurásico medio del Neuquén (Patagonia septentrional). Uno de los mas pequenosaurios conocidos. *Acta Congr. Argent. Paleontol. Bioestratigraf.* **2**, 87–102.
34. Codorniu L, Gasparini Z. 2013 The Late Jurassic pterosaurs from northern Patagonia, Argentina. *Earth Environ. Sci. Trans. R. Soc. Edinb.* **103**, 399–408. (doi:10.1017/S1755691013000388)
35. Figari EG, Scasso RA, Cúneo RN, Escapa I. 2015 Estratigrafía y evolución de la Cuenca de Cañadón Asfalto, provincia del Chubut, Argentina. *Lat. Am. J. Sedimentol. Basin Anal.* **22**, 135–169.
36. Figari EG, Courtade S. 1993 Evolución tectosedimentaria de la cuenca de Cañadón Asfalto, Chubut, Argentina. *XII Cong. Geol. Argent. y II Cong. Explor. Hidrocarb. Actas* **1**, 66–77.
37. Stipanovich PN, Rodrigo F, Baulies OL, Martínez CG. 1968 Las formaciones pre-senonianas en el denominado macizo nordpatagónico y regiones adyacentes. *Rev. Asoc. Geol. Arg.* **23**, 67–98.
38. Bonaparte JF. 1978 El Mesozoico de América del Sur y sus tetrápodos. In *Opera lilloana*, vol. 26. Ministerio de Cultura y Educación, Fundación Miguel Lillo.
39. Ardolino A, Franchi M, Remesal M, Salani F. 2008 Sitios de interés geológico, ed. servicio geológico minero argentino anales. In *La meseta de somún curá*, pp. 643–658.
40. Cúneo R, Ramezani J, Scasso R, Pol D, Escapa I, Zavattieri AM, Bowring SA. 2013 High-precision U–Pb geochronology and a new chronostratigraphy for the Cañadón Asfalto Basin, Chubut, central Patagonia: implications for terrestrial faunal and floral evolution in Jurassic. *Gondwana Res.* **24**, 1267–1275. (doi:10.1016/j.gr.2013.01.010)
41. Fantasia A, Föllmi KB, Adatte T, Spangenberg JE, Schoene B, Barker RT, Scasso RA. 2021 Late Toarcian continental palaeoenvironmental conditions: an example from the Cañadón Asfalto Formation in southern Argentina. *Gondwana Res.* **89**, 47–65. (doi:10.1016/j.gr.2020.10.001)
42. Cabaleri N, Volkheimer W, Nieto DS, Armella C, Cagnoni M, Hauser N, Matteini M, Pimentel MM. 2010 U–Pb ages in zircons from Las Chacritas and Puesto Almada members of the Jurassic Cañadón Asfalto Formation, Chubut province, Argentina. In *South American Symp. on Isotope Geology, Brasília*, Abstracts, pp. 190–193.
43. Rauhut OWM. 2007 A fragmentary theropod skull from the Middle Jurassic of Patagonia. *Ameghiniana* **44**, 479–483.
44. Sterli J. 2008 A new, nearly complete stem turtle from the Jurassic of South America with implications for turtle evolution. *Biol. Lett.* **4**, 286–289. (doi:10.1098/rsbl.2008.0022)
45. Apesteguía S, Gómez RO, Rougier GW. 2012 A basal spheodontian (Lepidosauria) from the Jurassic of Patagonia: new insights on the phylogeny and biogeography of Gondwanan rhynchocephalians. *Zool. J. Linn. Soc.* **166**, 342–360. (doi:10.1111/j.1096-3642.2012.00837.x)
46. Becerra MG, Pol D, Rauhut OWM, Cerda IA. 2016 New heterodontosaurid remains from the Cañadón Asfalto Formation: cursoriality and the functional importance of the pes in small heterodontosaurids. *J. Paleontol.* **90**, 555–577. (doi:10.1017/jpa.2016.24)
47. Carballido JL, Pol D, Otero A, Cerda IA, Salgado L, Garrido AC, Ramezani J, Cúneo NR, Krause JM. 2017 A new giant titanosaur sheds light on body mass evolution among sauropod dinosaurs. *Proc. R. Soc. B* **284**, 20171219. (doi:10.1098/rspb.2017.1219)
48. Gaetano LC, Rougier GW. 2012 First Amphilestid from South America: a Molariform from the Jurassic Cañadón Asfalto Formation, Patagonia, Argentina. *J. Mammal. Evol.* **19**, 235–248. (doi:10.1007/s10914-012-9194-1)

49. Rougier GW, Martinelli AG, Forasiepi AM, Novacek MJ. 2007 New Jurassic mammals from Patagonia, Argentina: a reappraisal of australosphenidan morphology and interrelationships. *Am. Museum Novitates* **3566**, 1. (doi:10.1206/0003-0082(2007)507[1:NUMFPA]2.0.CO;2)
50. Gaetano LC, Rougier GW. 2011 New materials of *Argentoconodon fariassorum* (Mammaliaformes, Triconodontidae) from the Jurassic of Argentina and its bearing on triconodont phylogeny. *J. Vertebr. Paleontol.* **31**, 829–843. (doi:10.1080/02724634.2011.589877)
51. Rauhut OWM. 2005 Osteology and relationships of a new theropod dinosaur from the Middle Jurassic of Patagonia. *Palaeontology* **48**, 87–110. (doi:10.1111/j.1475-4983.2004.00436.x)
52. Rauhut OWM, Pol D. 2019 Probable basal allosauroid from the early Middle Jurassic Cañadón Asfalto Formation of Argentina highlights phylogenetic uncertainty in tetanuran theropod dinosaurs. *Sci. Rep.* **9**, 18826. (doi:10.1038/s41598-019-53672-7)
53. Goloboff PA, Farris JS, Nixon KC. 2008 TNT, a free program for phylogenetic analysis. *Cladistics* **24**, 774–786. (doi:10.1111/j.1096-0031.2008.00217.x)
54. Goloboff PA, Morales ME. 2023 TNT version 1.6, with a graphical interface for MacOS and Linux, including new routines in parallel. *Cladistics* **39**, 144–153. (doi:10.1111/clad.12524)
55. Fernandes AE, Beccari V, Kellner AWA, Mateus O. 2023 A new gnathosaurine (Pterosauria, Archaeopterygoidea) from the Late Jurassic of Portugal. *PeerJ* **11**, e16048. (doi:10.7717/peerj.16048)
56. Andres B. 2021 Phylogenetic systematics of *Quetzalcoatlus* Lawson 1975 (Pterodactyloidea: Azhdarchoidea). *J. Vertebr. Paleontol.* **41**, 203–217. (doi:10.1080/02724634.2020.1801703)
57. Goloboff PA, Szumik CA. 2015 Identifying unstable taxa: efficient implementation of triplet-based measures of stability, and comparison with Phyutility and RogueNaRok. *Mol. Phylogenet. Evol.* **88**, 93–104. (doi:10.1016/j.ympev.2015.04.003)
58. Pol D, Escapa IH. 2009 Unstable taxa in cladistic analysis: identification and the assessment of relevant characters. *Cladistics* **25**, 515–527. (doi:10.1111/j.1096-0031.2009.00258.x)
59. Owen R. 1842 Report on British fossil reptiles, Part II. In *Proc. 11th Meeting of the British Association for the Advancement of Science*, Plymouth, UK, pp. 60–204.
60. Fernández Garay A. 2004 *Diccionario tehuelche-español/índice español-tehuelche*. Leiden, The Netherlands: CNWS Research School of Asian, African and Amerindian Studies, University of Leiden.
61. Wellnhofer P. 1978 Pterosauria. In *Handbuch der paläoherpertologie, encyclopedia of paleoherpertology*, 19 (ed. P Wellnhofer), pp. 1–82. Stuttgart, Germany: Fischer-Verlag.
62. Wellnhofer P. 1991 *The illustrated encyclopedia of pterosaurs*. London, UK: Salamander Books.
63. Kellner AW. 2003 Pterosaur phylogeny and comments on the evolutionary history of the group. In *Evolution and palaeobiology of pterosaurs*, vol. 217 (eds E Buffetaut, JM Mazin), pp. 1–3. London, UK: Geological Society. (doi:10.1144/GSL.SP.2003.217.01.01)
64. Andres B, Qiang J. 2008 A new pterosaur from the Liaoning Province of China, the phylogeny of the Pterodactyloidea, and convergence in their cervical vertebrae. *Palaeontology* **51**, 453–469. (doi:10.1111/j.1475-4983.2008.00761.x)
65. Wellnhofer P. 1975 Die rhamphorhynchoidea (pterosauria) der oberjura-plattenkalke süddeutschlands. *Palaeontogr. A* **149**, 1–30.
66. Cheng X, Jiang S, Wang X, Kellner AWA. 2017 New anatomical information of the wukongopterid *Kunpengopteris sinensis* Wang et al., 2010 based on a new specimen. *PeerJ* **5**, e4102. (doi:10.7717/peerj.4102)
67. Lü JC, Xu L, Chang H, Zhang X. 2011 A new darwinopterid pterosaur from the Middle Jurassic of western Liaoning, northeastern China and its ecological implications. *Acta Geol. Sin. Eng. Ed.* **85**, 507–514.
68. Unwin DM, Lü J. 2013 The basal monofenestratan *Darwinopteris* and its implication for the origin and basal radiation of pterodactyloid pterosaurs. In *Int. Symp. on Pterosaurs, Rio de Janeiro, Argentina*, short communications, pp. 98–101.
69. Sangster S. 2021 The osteology of *Dimorphodon macronyx*, a non-pterodactyloid pterosaur from the Lower Jurassic of Dorset, England. *Monogr. Palaeontogr. Soc.* **175**, 1–48. (doi:10.1080/02693445.2021.2037868)
70. Padian K. 2008 The Early Jurassic pterosaur *Campylognathoides* Strand, 1928. In *Special papers in palaeontology*, vol. 80, pp. 65–107.
71. Padian K. 2008 The Toarcian (Early Jurassic) pterosaur *Dorygnathus* Wagner, 1860. *Palaeontology* **80**, 1–64.
72. Bennett SC. 2012 The morphology and taxonomy of the pterosaur *Cynorhamphus*. *Neues Jahrb. Geol. Paläontol. Abh.* **267**, 23–41. (doi:10.1127/0077-7749/2012/0295)
73. Plieninger F. 1901 Beiträge zur Kenntnis der Flugsaurier. *Palaeontographica* **48**, 65–90.
74. Nopsca F. 1928 The genera of reptiles. *Palaeobiologica* **1**, 163–188. (doi:10.2534/jjasnaoe1903.1928.163)
75. Fastnacht M. 2005 Jaw mechanics of the pterosaur skull construction and the evolution of toothlessness. PhD thesis, Johannes Gutenberg-Universität, Mainz, Germany.
76. Hoffmann R, Bestwick J, Berndt G, Berndt R, Fuchs D, Klug C. 2020 Pterosaurs ate soft-bodied cephalopods (Coleoidea). *Sci. Rep.* **10**, 1230. (doi:10.1038/s41598-020-57731-2)
77. Martill D, Etches S. 2012 A new monofenestratan pterosaur from the Kimmeridge Clay Formation (Kimmeridgian, Upper Jurassic) of Dorset, England. *Acta Palaeontol. Pol.* **58**, 285–295. (doi:10.4202/app.2011.0071)
78. O'Sullivan M, Martill DM. 2015 Evidence for the presence of *Rhamphorhynchus* (Pterosauria: Rhamphorhynchinae) in the Kimmeridge Clay of the UK. *Proc. Geol. Assoc.* **126**, 390–401. (doi:10.1016/j.pgeola.2015.03.003)
79. Wang XL, Kellner AWA, Jiang SX, Cheng X, Meng X, Rodrigues T. 2010 Longtailed pterosaurs (Wukongopteridae) from western Liaoning, China. *Anais. Acad. Bras. Ciênc.* **82**. (doi:10.1590/S0001-37652010000400024)
80. Padian K. 1984 *Osteology and functional morphology of Dimorphodon macronyx* (Buckland) (Pterosauria: Rhamphorhynchoidea) based on new material in the Yale Peabody Museum. New Haven, CT: Peabody Museum of Natural History.

81. Owen R. 1859 On a new genus (*Dimorphodon*) of pterodactyle, with remarks on the geological distribution of flying reptiles. *Rep. Brit. Assoc. Adv. Sci.* **28**, 97–103.
82. Bennett SC. 2014 A new specimen of the pterosaur *Scaphognathus crassirostris*, with comments on constraint of cervical vertebrae number in pterosaurs. *Neues Jahrb. Geol. Paläontol. Abh.* **271**, 327–348. (doi:10.1127/0077-7749/2014/0392)
83. Cheng X, Wang X, Jiang S, Kellner AWA. 2012 A new scaphognathid pterosaur from western Liaoning, China. *Hist. Biol.* **24**, 101–111. (doi:10.1080/08912963)
84. Witmer LM, Chatterjee S, Franzosa J, Rowe T. 2003 Neuroanatomy of flying reptiles and implications for flight, posture and behaviour. *Nature* **425**, 950–953. (doi:10.1038/nature02048)
85. He X, Yan D, Su C. 1983 A new pterosaur from the Middle Jurassic of Dashanpu, Zigong, Sichuan. *J. Chengdu Coll. Geol.* 27–33.
86. O'Sullivan M, Martill DM. 2017 The taxonomy and systematics of *Parapsicephalus purdoni* (Reptilia: Pterosauria) from the Lower Jurassic Whitby Mudstone Formation, Whitby, UK. *Hist. Biol.* **29**, 1009–1018. (doi:10.1080/08912963.2017.1281919)
87. Wellnhofer P. 1970 Die Pterodactyloidea (Pterosauria) der Oberjura-Plattenkalke Süddeutschlands. *Abh. d. Math.-Phys. Kl. d. Königl. Bayer. Akad. d. Wiss.* **141**, 1–133.
88. Bennett SC. 2001 The osteology and functional morphology of the Late Cretaceous pterosaur *Pteranodon*. Part I. General description of osteology. *Palaeontographica* **260**, 1–112. (doi:10.1127/pala/260/2001/1)
89. Bennett SC. 2021 Complete large skull of the pterodactyloid pterosaur *Ctenochasma elegans* from the Late Jurassic Solnhofen Lithographic Limestones. *Neues Jahrb. Geol. Paläontol. Abh.* **301**, 283–294. (doi:10.1127/njgpa/2021/1011)
90. Beccari V, Pinheiro FL, Nunes I, Anelli LE, Mateus O, Costa FR. 2021 Osteology of an exceptionally well-preserved tapejarid skeleton from Brazil: revealing the anatomy of a curious pterodactyloid clade. *PLoS ONE* **16**, e0254789. (doi:10.1371/journal.pone.0254789)
91. Witton MP, O'Sullivan M, Martill DM. 2015 The relationships of *Cuspicephalus scarfi* Martill and Etches, 2013 and *Normannognathus wellnhoferi* Buffetaut et al. 1998 to other monofenestratan pterosaurs. *Contrib. Zool.* **84**, 115–127.
92. Zhou CF, Gao KQ, Yi H, Xue J, Li Q, Fox RC. 2017 Earliest filter-feeding pterosaur from the Jurassic of China and ecological evolution of Pterodactyloidea. *R. Soc. Open Sci.* **4**, 160672. (doi:10.1098/rsos.160672)
93. Navarro CA, Martin-Silverstone E, Stubbs TL. 2018 Morphometric assessment of pterosaur jaw disparity. *R. Soc. Open Sci.* **5**, 172130. (doi:10.1098/rsos.172130)
94. Bestwick J, Unwin DM, Butler RJ, Henderson DM, Purnell MA. 2018 Pterosaur dietary hypotheses: a review of ideas and approaches. *Biol. Rev.* **93**, 2021–2048. (doi:10.1111/brv.12431)
95. Moser M, Rauhut OWM. 2011 Der reusengebiss-flugsaurier ctenochasma fossilien sonderheft, 47–48.
96. Bestwick J, Unwin DM, Butler RJ, Purnell MA. 2020 Dietary diversity and evolution of the earliest flying vertebrates revealed by dental microwear texture analysis. *Nat. Commun.* **11**, 5293. (doi:10.1038/s41467-020-19022-2)
97. Upchurch P, Andres B, Butler RJ, Barrett PM. 2015 An analysis of pterosaurian biogeography: implications for the evolutionary history and fossil record quality of the first flying vertebrates. *Hist. Biol.* **27**, 697–717. (doi:10.1080/08912963.2014.939077)
98. Fernandes AE, Pol D, Rauhut O. 2024 Supplementary material from: The oldest monofenestratan pterosaur from the Queso Rallado locality (Cañadón Asfalto Formation, Toarcian) of Chubut province, Patagonia, Argentina. Figshare. (doi:10.6084/m9.figshare.c.7550725)